

## Chapter 2

### Review of Time Domain TLM

In 1971, Johns and Beurl introduced a novel numerical technique for solving 2-D scattering problems. The technique was originally based on Huygen's model of wave propagation and inspired by earlier network simulation techniques.

According to Huygen's principle, a wave front consists of a number of secondary radiators that give rise to spherical wavelets. The envelope of these wavelets forms a new wavefront which in turns give rise to spherical wavelets and so on.

In order to discretize Huygen's principle in a 2-D space, both space and time are represented in terms of finite elementary units  $\Delta\ell$  and  $\Delta t$ . The 2-D space is modeled by a cartesian matrix of points or nodes separated by a mesh spacing  $\Delta\ell$ , the time  $\Delta t$  is the time it takes the pulse to travel from one node to the next. Assuming an impulse incident upon one of the nodes as shown in Figure (2.1a) and the energy of the impulse is unity. According to Huygen's principle, the energy will be isotropically scattered in all directions, each direction should carry one fourth of the energy, or in terms of field quantities each should be  $1/2$  in magnitude. To insure field continuity, the reflected pulse at port one should have a reflection coefficient of  $-1/2$ . The 2 dimensional model can be represented in terms of a network model that can be thought of as a mesh of orthogonal transmission lines interconnected at the nodes shown in Figure (2.1b). Assuming an incident pulse of 1 volt, the pulse will be partially reflected and partially transmitted according to the transmission line theory. If all the lines

have the same characteristic impedance  $Z$ , then the equivalent impedance seen by the incident pulse will be  $Z/3$ , the corresponding reflection coefficient  $\Gamma$  will be  $-1/2$  and the transmission coefficient  $\tau$  will be  $1/2$ . Therefore the scattered pulse at ports 2,3 and 4 will be  $1/2$  and that at port 1 will be  $1/2$ . The scattered pulses continue to propagate to be incident on adjacent nodes and so on.

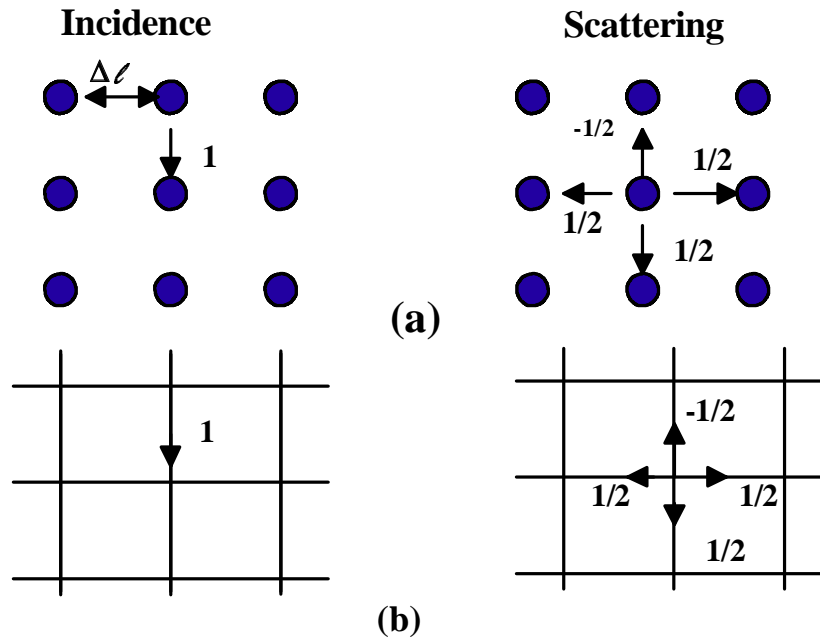


Figure 2.1

a- Discretized Huygen's principle

b- Equivalent transmission line model

## 2.1 The series TLM node

The series TLM node is suitable for solving 2-D problems with only three nonzero field components, one magnetic field component  $H_z$  and two electric field components  $E_x$  and  $H_y$ . The series TLM node also assumes no field variations along the  $z$  direction. The circuit structure of the series node is shown in Figure (2.2). From the above assumptions, the associated Maxwell's equations will be

$$\frac{\partial H_z}{\partial y} = \epsilon \frac{\partial E_x}{\partial t} \quad (2.1a)$$

$$-\frac{\partial H_z}{\partial x} = \epsilon \frac{\partial E_y}{\partial t} \quad (2.1b)$$

$$\frac{\partial E_y}{\partial x} - \frac{\partial E_x}{\partial y} = -\mu \frac{\partial H_z}{\partial t} \quad (2.1c)$$

The relation between circuit quantities and field quantities are derived in [4] and are given by

$$H_z = \frac{I_z}{\Delta z} \quad (2.2a)$$

$$E_y = -\frac{V_y}{\Delta y} \quad (2.2b)$$

$$E_x = -\frac{V_x}{\Delta x} \quad (2.2c)$$

Scattering in a series node can be easily derived from the Thevenin's equivalent circuit model. Each transmission line is replaced by its Thevenin's equivalent which is an equivalent impedance equal to the intrinsic impedance of the line and an equivalent open circuited voltage equal to twice the incident voltage. The Thevenin's equivalent circuit is shown in Figure (2.3).

The loop current  $I_k$  can be obtained from the Thevenin's equivalent as

$$I_k = \frac{2_k V_1^i + 2_k V_4^i - 2_k V_3^i - 2_k V_2^i}{4Z} \quad (2.3)$$

The reflected voltages can then be obtained as

$${}_k V_1^r = {}_k V_1 - {}_k V_1^i = 2_k V_1^i - I_k Z - {}_k V_1^i \quad (2.4)$$

substituting for  $I_k$  from equation (2.3) yields

$${}_k V_1^r = \frac{1}{2}({}_k V_1^i + {}_k V_2^i + {}_k V_3^i - {}_k V_4^i) \quad (2.5)$$

Similar expressions for the scattered voltages at other ports can be obtained in the same way. The resulting scattering matrix will have the form

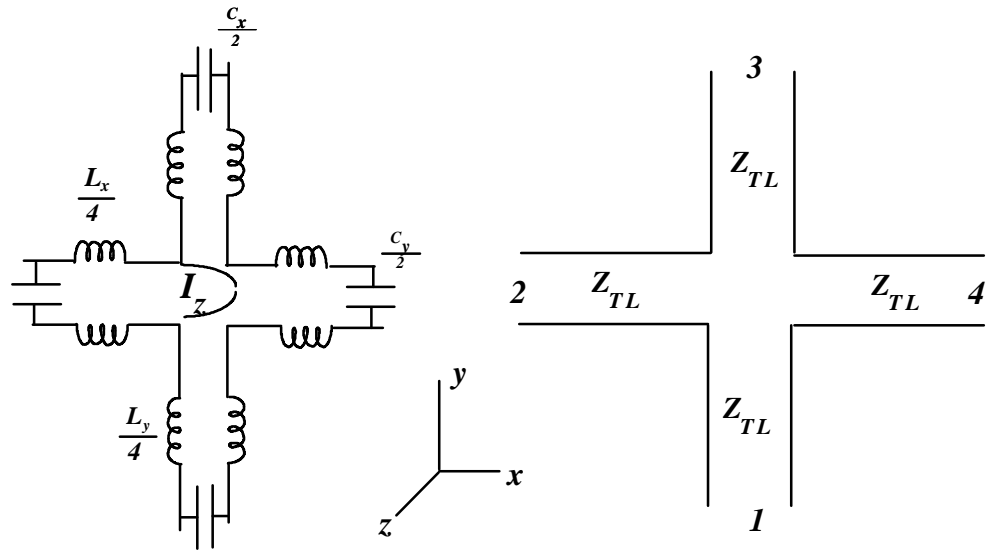


Figure 2.2

a - The series TLM node      b - Equivalent transmission line model

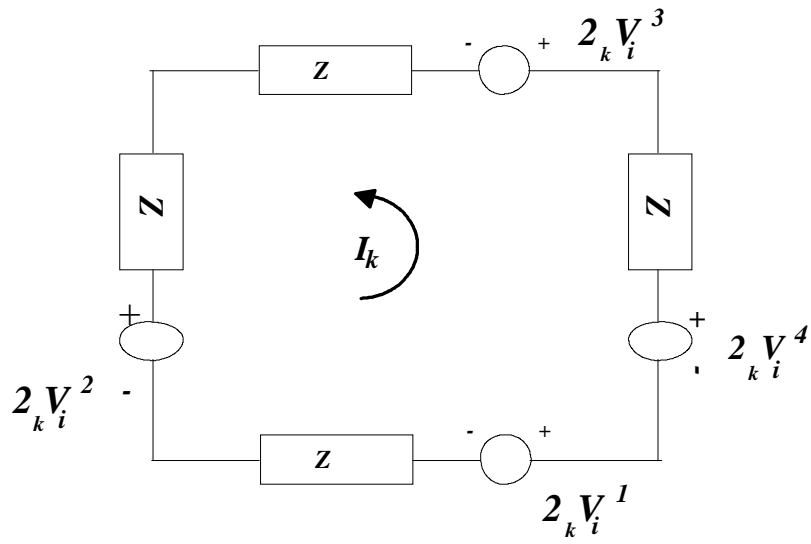


Figure 2.3 Thevenin's equivalent circuit model for the series node

$$\begin{bmatrix} {}_k V_1^r \\ {}_k V_2^r \\ {}_k V_3^r \\ {}_k V_4^r \end{bmatrix} = \frac{1}{2} \begin{bmatrix} 1 & 1 & 1 & -1 \\ 1 & 1 & -1 & 1 \\ 1 & -1 & 1 & 1 \\ -1 & 1 & 1 & 1 \end{bmatrix} \begin{bmatrix} {}_k V_1^i \\ {}_k V_i^r \\ {}_k V_i^r \\ {}_k V_i^r \end{bmatrix} \quad (2.6)$$

Following the scattering procedure is the connection procedure where the reflected voltage at each port becomes incident on the neighboring port at the next time step. The connection procedure can be expressed as

$${}_{k+1} V_1^i(x, y) = {}_k V_3^r(x, y - 1) \quad (2.7a)$$

$${}_{k+1} V_2^i(x, y) = {}_k V_4^r(x - 1, y) \quad (2.7b)$$

$${}_{k+1} V_3^i(x, y) = {}_k V_1^r(x, y + 1) \quad (2.7c)$$

$${}_{k+1} V_4^i(x, y) = {}_k V_2^r(x + 1, y) \quad (2.7d)$$

In a series TLM node, the link line impedances are chosen to be the same and equal to the intrinsic impedance of free space. In order to model a medium of permeability different from that of free space, a short circuited series stub of length  $\Delta\ell/2$  and characteristic impedance  $Z$  is used to compensate for the deficiency in inductance. A matched series stub can also be used to account for magnetic losses [4]. The scattering matrix of a series node with open circuited and matched stubs can simply be derived by adding the corresponding elements to the Thevenin's equivalent circuit in Figure 2.3 and using the same exact procedure as with the stubless series node.

## 2.2 The shunt TLM node

The shunt node is capable of modeling wave propagation in a 2-D space. It is suitable for problems with only three nonzero field components which are one electric field component  $E_z$  and two magnetic field components  $H_x$  and  $H_y$  (TM modes). The Maxwell's equations corresponding to a TM mode are

$$\frac{\partial E_z}{\partial y} = -\mu \frac{\partial H_x}{\partial t} \quad (2.8a)$$

$$\frac{\partial E_z}{\partial x} = -\mu \frac{\partial H_y}{\partial t} \quad (2.8b)$$

$$\frac{\partial H_y}{\partial x} - \frac{\partial H_x}{\partial y} = -\epsilon \frac{\partial E_z}{\partial t} \quad (2.8c)$$

The transmission line model of the shunt node and the equivalent Thevenin's circuit model is shown in Figure (2.4)

The scattering matrix of the shunt node can be obtained using the Thevenin's equivalent circuit model and a similar procedure to that used in the series node. In the shunt node, all link line impedances are chosen to be the same equal to the intrinsic impedance of free space. To model a medium of relative permeability different from free space, shunt open circuited stubs are added to compensate the deficiency in capacitance. Shunt matched stubs can also be used to model electric losses.

It is worth mentioning that from the principle of duality, both the shunt and series nodes can be used to simulate either TE or TM modes by making the appropriate analogy between field and circuit quantities.

### 2.3 The Expanded node

The series and shunt nodes discussed above are capable of simulating wave propagation in a 3-D space. However, because most problems encountered in engineering applications are 3-D, it became essential to extend the TLM to 3-D space to form a network that can model three electric and three magnetic field components.

The first 3-D node introduced was the expanded node [5]. The expanded node was obtained by the appropriate combination of the series and shunt nodes as shown in Figure (2.5). A series node on the x-z plane connected to two shunt nodes in the y-z and x-y plane and a shunt node in the x-z plane connected to series nodes on the y-z and x-y plane. The disadvantage of this node lies mainly in its complexity. Also, when making the analogy between circuit and field components, it was found that different field components with different polarization were calculated at points that were physically separated which made it difficult to apply boundary conditions.

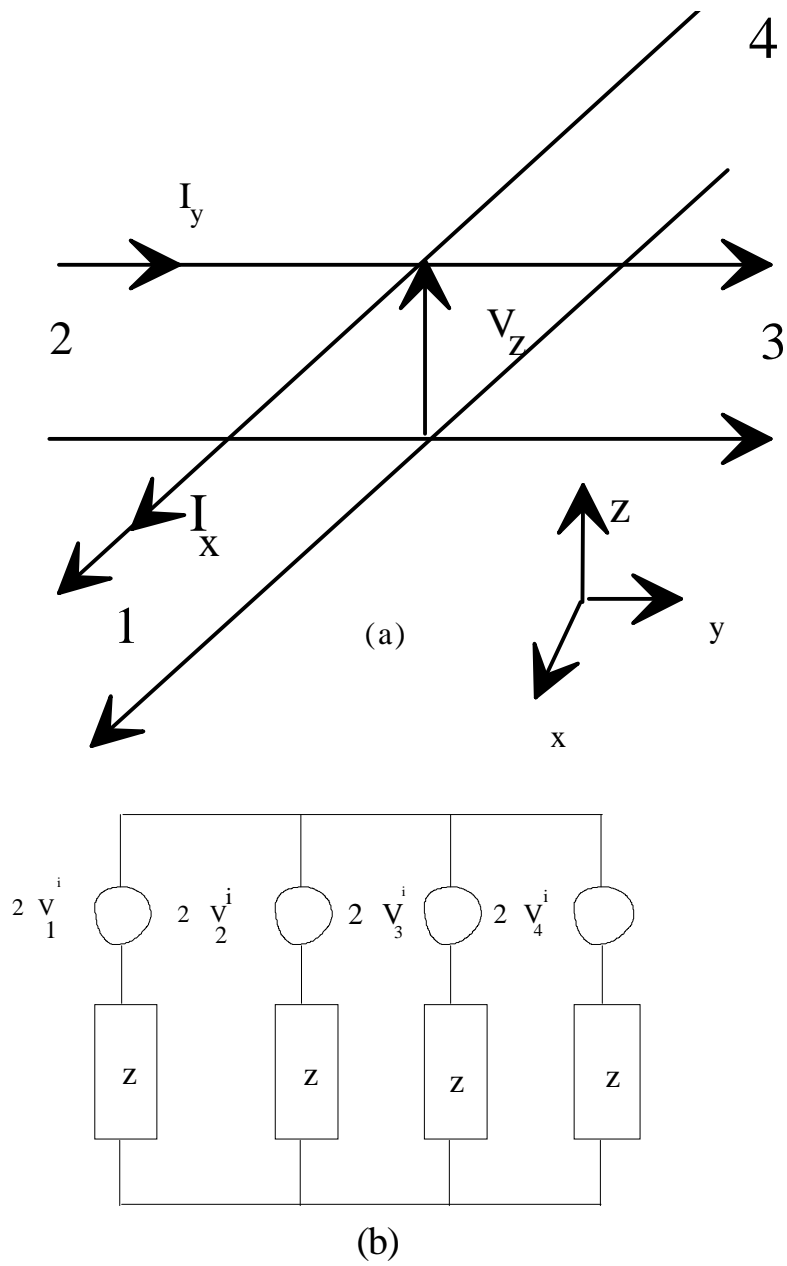


Figure 2.4

a- The shunt TLM node

b- Thevenin's equivalent circuit model

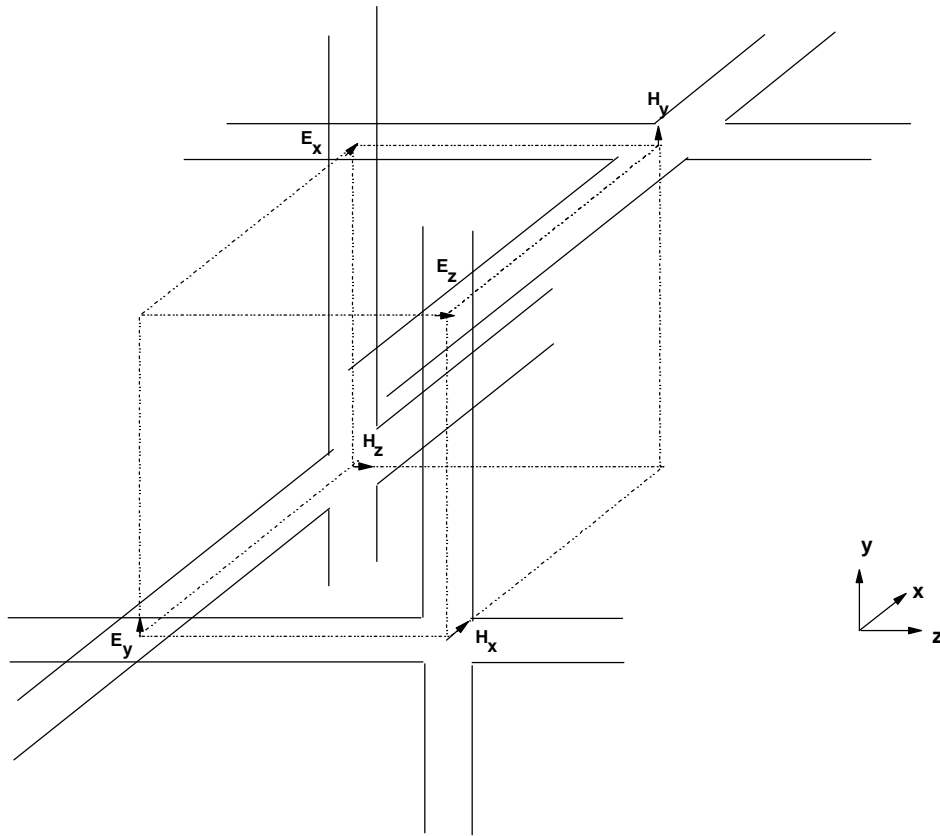


Figure 2.5 The expanded node

## 2.4 The Symmetrical condensed node (SCN)

The symmetrical condensed node consists of 12 ports to represent two polarization in each coordinate direction as demonstrated in Figure 2.6. The voltage pulses corresponding to two polarizations are carried on transmission line pairs. The correspondence between the electromagnetic field components and the voltages and currents on the transmission lines as given by [6] can be written as



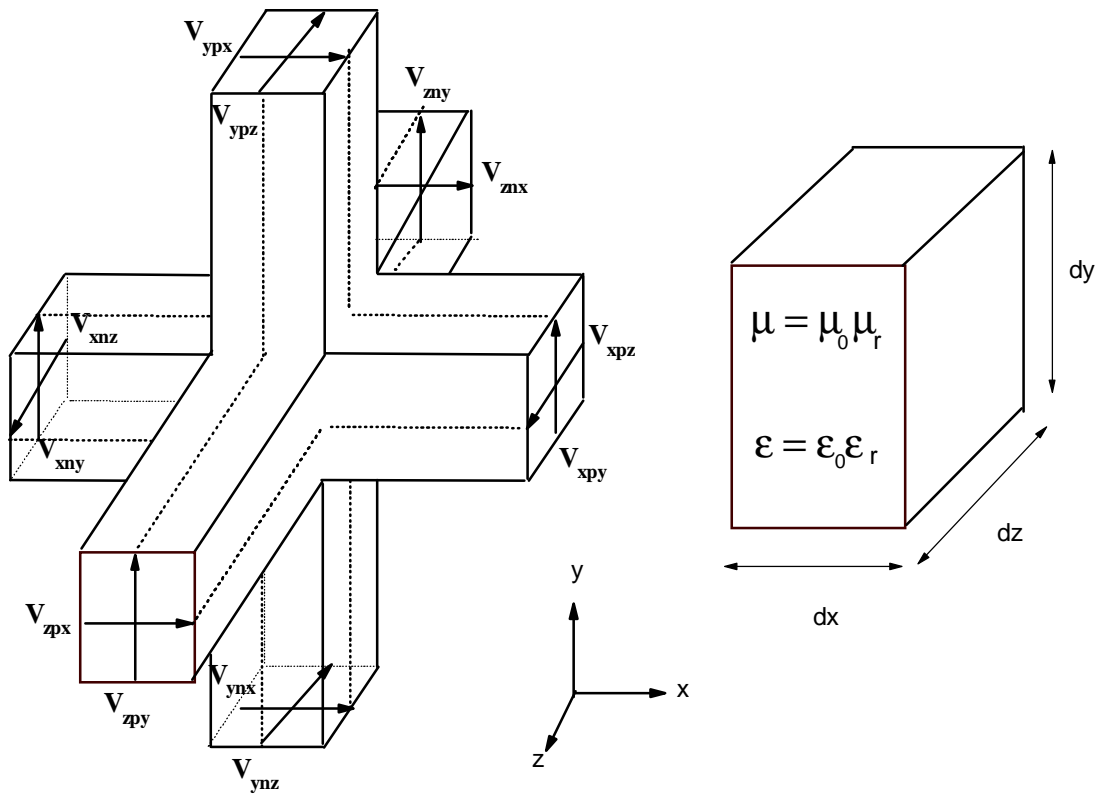


Figure 2.6 The Symmetrical condensed node

$$E_x = -\frac{V_x}{\Delta x}, \quad E_y = -\frac{V_y}{\Delta y}, \quad E_z = -\frac{V_z}{\Delta z}, \quad (2.9)$$

$$H_x = \frac{I_x}{\Delta x}, \quad H_y = \frac{I_y}{\Delta y}, \quad H_z = \frac{I_z}{\Delta z} \quad (2.10)$$

For a medium with permittivity  $\epsilon$  and permeability  $\mu$  simulated by a mesh of cell dimensions  $\Delta x$ ,  $\Delta y$ , and  $\Delta z$ , the overall capacitance in the x, y and z directions associated with an  $E_x$ ,  $E_y$  and  $E_z$  polarization, respectively, are given by

$$C_x = \epsilon \frac{\Delta y \Delta z}{\Delta x} \quad C_y = \epsilon \frac{\Delta x \Delta z}{\Delta y} \quad C_z = \epsilon \frac{\Delta y \Delta x}{\Delta z} \quad (2.11)$$

Similarly, the overall inductances in the x, y, and z direction are given by

$$L_x = \mu \frac{\Delta y \Delta z}{\Delta x} \quad L_y = \mu \frac{\Delta x \Delta z}{\Delta y} \quad L_z = \mu \frac{\Delta y \Delta x}{\Delta z} \quad (2.12)$$

#### 2.4.1 The SCN in an inhomogeneous medium

In the symmetrical condensed node, all the link line impedances are chosen to be the same and equal to the intrinsic impedance of free space  $Z_0$ . Consequently, the capacitance and inductance of each link line are given by

$$C = \frac{\Delta t/2}{Z_0}, \quad L = \frac{\Delta t}{2} Z_0 \quad (2.13)$$

where  $\Delta t$  is the time step on the mesh or the delay along a transmission line section of length  $\Delta \ell$  (the size of the mesh). If the overall capacitances and inductances of the link lines do not exactly model the local material parameters, the capacitance and/or inductance deficiency are compensated for through the use of open circuited and/or short circuited stubs, respectively. In order to exactly model the medium parameters  $\epsilon$  and  $\mu$ , the following set of equations have to be satisfied for the link line capacitance and inductance

$$L_x = \mu \frac{\Delta y \Delta z}{\Delta x} = L_{dyz} \Delta y + L_{dzy} \Delta z \quad (2.14.a)$$

$$L_y = \mu \frac{\Delta x \Delta z}{\Delta y} = L_{dxz} \Delta x + L_{dzx} \Delta z \quad (2.14.b)$$

$$L_z = \mu \frac{\Delta y \Delta x}{\Delta z} = L_{dyx} \Delta y + L_{dxy} \Delta x \quad (2.14.c)$$

$$C_x = \epsilon \frac{\Delta y \Delta z}{\Delta x} = C_{dyx} \Delta y + L_{dzx} \Delta z \quad (2.14.d)$$

$$C_y = \epsilon \frac{\Delta z \Delta x}{\Delta y} = C_{dxy} \Delta x + L_{dzy} \Delta z \quad (2.14.e)$$

$$C_z = \epsilon \frac{\Delta y \Delta x}{\Delta z} = C_{dyz} \Delta y + C_{dxz} \Delta x \quad (2.14.f)$$

where the first subscript d indicates normalized quantities per unit length, the second subscript indicates line direction and the third for polarization. Substituting for every link line inductance and capacitance in terms of the link line impedance and delay from equation (2.13), the above set of equations can be written as

$$\mu S_x = \Delta t (Z_{yz} + Z_{zy}) \quad (2.15.a)$$

$$\mu S_y = \Delta t (Z_{xz} + Z_{zx}) \quad (2.15.b)$$

$$\mu S_z = \Delta t (Z_{yx} + Z_{xy}) \quad (2.15.c)$$

$$\epsilon S_x = \Delta t (Y_{yx} + Y_{zx}) \quad (2.15.d)$$

$$\epsilon S_y = \Delta t (Y_{xy} + Y_{zy}) \quad (2.15.e)$$

$$\epsilon S_z = \Delta t (Y_{xz} + Y_{yz}) \quad (2.15.f)$$

where  $S_x = \frac{\Delta y \Delta z}{\Delta x}$     $S_y = \frac{\Delta x \Delta z}{\Delta y}$     $S_z = \frac{\Delta y \Delta x}{\Delta z}$   
and  $Z_{rq} = \frac{1}{Y_{rq}}$    r, q can be x, y or z

For the SCN,  $Z_{xy} = Z_{yx} = Z_{yz} = Z_{zy} = Z_{zx} = Z_{xz} = Z_0$ , therefore, from equations (2.14a) and (2.15a), the deficiency in inductance in the x direction is given by

$$L_x^s = \mu S_x - 4 \left( \frac{\Delta t}{2} \right) Z_0 \quad (2.16)$$

the deficiency in inductance in the x direction is compensated by a short circuit stub of characteristic impedance given by

$$Z_x^s = \frac{L_x^s}{\Delta t/2} = 2\mu \frac{S_x}{\Delta t} - 4Z_0 \Rightarrow \hat{Z}_x^s = \frac{Z_x^s}{Z_0} = \frac{2\mu_r S_x}{c_0 \Delta t} - 4, \quad c_0 = \frac{1}{\sqrt{\mu_0 \epsilon_0}} \quad (2.17)$$

Similarly, the normalized impedance of the short circuited stubs used to compensate for inductance deficiency in the y and z directions are given by

$$\hat{Z}_y^s = \frac{Z_y^s}{Z_0} = \frac{2\mu_r S_y}{c_0 \Delta t} - 4 \quad (2.18)$$

$$\hat{Z}_z^s = \frac{Z_z^s}{Z_0} = \frac{2\mu_r S_z}{c_0 \Delta t} - 4 \quad (2.19)$$

The deficiency of the capacitance in the x direction can be calculated as

$$C_x^s = \epsilon S_x - 4\left(\frac{\Delta t}{2}\right)Y_0 \quad (2.20)$$

and the admittance of the open circuited stub used to compensate for the deficiency in the x directed capacitance is given by

$$Y_x^s = \frac{C_x^s}{\Delta t/2}, \quad \hat{Y}_x^s = \frac{Y_x^s}{Y_0} = \frac{2\epsilon_r S_x}{c_0 \Delta t} - 4 \quad (2.21)$$

similarly, those in the y and z direction have normalized admittances given by

$$\hat{Y}_y^s = \frac{Y_y^s}{Y_0} = \frac{2\epsilon_r S_y}{c_0 \Delta t} - 4 \quad (2.22)$$

$$\hat{Y}_z^s = \frac{Y_z^s}{Y_0} = \frac{2\epsilon_r S_z}{c_0 \Delta t} - 4 \quad (2.23)$$

#### 2.4.2 Time step in the symmetrical condensed node

In order to guarantee the stability of a TLM mesh, all stub impedances or admittances must be positive. Unfortunately, this sets a hard limit on the maximum permissible time step for the mesh. For a generally graded mesh, and from equation (2.17) to (2.23), the maximum permissible time step is given by

$$\Delta t_{\max} = \min\left(\frac{\epsilon_r S_x}{2c_0}, \frac{\epsilon_r S_y}{2c_0}, \frac{\epsilon_r S_z}{2c_0}, \frac{\mu_r S_x}{2c_0}, \frac{\mu_r S_y}{2c_0}, \frac{\mu_r S_z}{2c_0}\right) \quad (2.24)$$

### 2.5 The Hybrid Symmetrical Condensed node (HSCN)

In the SCN discussed in the previous section, stability conditions sets a constraint on the maximum permissible time step on the mesh. From equation (2.24), it appears that this constraint is determined by the ratio between the largest and the smallest grid dimension. This implies that, in large problems, where large ratios are used to minimize storage, the time step can become very small resulting in long computational runs. In the HSCN [7,8], the

condition that all link lines should have the same impedance is relaxed. The characteristic impedance of the lines are varied to account for various mesh grading and to model some of the medium parameters. As a result, the number of stubs required is reduced than in the SCN which directly implies improved dispersive properties over the stub loaded SCN. The HSCN may also have larger time step as compared to the SCN in some instants and thus reducing the overall computational time. The HSCN was first introduced by *Scaramuzza and Lowery* [7] where the characteristic impedance of all link lines are chosen to model the right inductance required by the medium. The capacitance of the lines are then chosen to maintain synchronism in the three coordinate directions. Deficiency in capacitance are then accounted for through the use of open circuited stubs with the appropriate characteristic admittance. This node was later referred to as type I HSCN. In 1994, a complementary HSCN was introduced by *Berini and Wu* [8] referred to as type II HSCN. In this node the link line admittance are chosen to model all the required capacitance by the medium and the inductance are chosen to achieve synchronism. The deficiency in inductance is then accounted for through the use of short circuited stubs with the appropriate characteristic impedance.

### 2.5.1 Type I HSCN

In type I HSCN, equations (2.14.a - c) are exactly satisfied by choosing the characteristic impedance of all link lines associated with the same current to be the same. From equations (2.14.a) and (2.13), the above condition implies

$$L_{yz} = L_{dzy}\Delta z = L_{dyz}\Delta y = \mu \frac{S_x}{2} \quad (2.25.a)$$

similarly

$$L_{zx} = L_{dxz}\Delta x = L_{dzx}\Delta z = \mu \frac{S_y}{2} \quad (2.25.b)$$

$$L_{yx} = L_{dxy}\Delta x = L_{dyx}\Delta y = \mu \frac{S_z}{2} \quad (2.25.c)$$

The link line impedances are then given by

$$Z_{yz} = Z_{zy} = Z_x = \mu \frac{S_x}{2\Delta t} \quad (2.26.a)$$

$$Z_{xz} = Z_{zx} = Z_y = \mu \frac{S_y}{2\Delta t} \quad (2.26.b)$$

$$Z_{yx} = Z_{xy} = Z_z = \mu \frac{S_z}{2\Delta t} \quad (2.26.c)$$

The capacitance are chosen to maintain synchronism and are given by

$$C_{zy} = C_{yz} = \frac{\Delta t}{Z_x} = \frac{2\Delta t^2}{\mu S_x} \quad (2.27.a)$$

$$C_{zx} = C_{xz} = \frac{\Delta t}{Z_y} = \frac{2\Delta t^2}{\mu S_y} \quad (2.27.b)$$

$$C_{zy} = C_{yz} = \frac{\Delta t}{Z_x} = \frac{2\Delta t^2}{\mu S_x} \quad (2.27.c)$$

The deficiency of capacitance in the x direction is given by

$$C_x^s = \epsilon S_x - C_{yx} - C_{zx} = \epsilon S_x - 2\frac{\Delta t^2}{\mu}(S_z + S_y) \quad (2.28)$$

The normalized admittance of the open circuited stub in the x direction is given by

$$\hat{Y}_{ox}^s = \frac{1}{\sqrt{\frac{\epsilon_0}{\mu_0}}} \frac{C_x^s}{\Delta t/2} = \frac{2}{\sqrt{\frac{\epsilon_0}{\mu_0}}} \left( \epsilon \frac{S_x}{\Delta t} - 2\frac{\Delta t}{\mu}(S_y + S_z) \right) \quad (2.29.a)$$

Similarly in the y and z direction

$$\hat{Y}_{oy}^s = \frac{2}{\sqrt{\frac{\epsilon_0}{\mu_0}}} \left( \epsilon \frac{S_y}{\Delta t} - 2\frac{\Delta t}{\mu}(S_x + S_z) \right) \quad (2.29.b)$$

$$\hat{Y}_{oz}^s = \frac{2}{\sqrt{\frac{\epsilon_0}{\mu_0}}} \left( \epsilon \frac{S_z}{\Delta t} - 2\frac{\Delta t}{\mu}(S_x + S_y) \right) \quad (2.29.c)$$

Again, to guarantee stability of the TLM mesh, all stub admittances must be positive which consequently implies an upper limit on the time step for the HSCN. The limit is given by

$$\Delta t_{\max}^2 = \min \left( \mu \epsilon \frac{S_x}{S_y + S_z}, \mu \epsilon \frac{S_y}{S_x + S_z}, \mu \epsilon \frac{S_z}{S_y + S_x} \right) \quad (2.30)$$

### 2.5.2 Type II HSCN

Type II HSCN is exactly the complement of type I HSCN where equations (2.14.e - f) are exactly satisfied by choosing the characteristic admittance of all link lines associated with the same electric field to be the same. The inductances are chosen to achieve synchronism. Deficiency in inductance is then compensated through the use of short circuited stubs. From equations (2.14 e -f) and (2.13), the link line admittances can be written as

$$Y_{yx} = Y_{zx} = Y_x = \epsilon \left( \frac{S_x}{2\Delta t} \right) \quad (2.31a)$$

$$Y_{xy} = Y_{zy} = Y_y = \epsilon \left( \frac{S_y}{2\Delta t} \right) \quad (2.31b)$$

$$Y_{xz} = Y_{yz} = Y_z = \left( \epsilon \frac{S_z}{2\Delta t} \right) \quad (2.31c)$$

By analogy with type I HSCN, the normalized impedances of the short circuited stubs in the x, y and z directions can be expressed as

$$Z_{ox}^s = \frac{2}{\sqrt{\frac{\mu_0}{\epsilon_0}}} \left( \mu \frac{S_x}{\Delta t} - 2 \frac{\Delta t}{\epsilon} (S_y + S_z) \right) \quad (2.32a)$$

$$Z_{oy}^s = \frac{2}{\sqrt{\frac{\mu_0}{\epsilon_0}}} \left( \mu \frac{S_y}{\Delta t} - 2 \frac{\Delta t}{\epsilon} (S_x + S_z) \right) \quad (2.32b)$$

$$Z_{oz}^s = \frac{2}{\sqrt{\frac{\mu_0}{\epsilon_0}}} \left( \mu \frac{S_z}{\Delta t} - 2 \frac{\Delta t}{\epsilon} (S_y + S_x) \right) \quad (2.32c)$$

The same constraint for the maximum allowable time step for the type I HSCN still applies for type II HSCN.

## 2.6 The Symmetrical Super Condensed node SSCN

In the HSCN, it was found that by allowing the characteristic impedance of the link lines to be different ( three different link line impedances were used), the number of stubs can be reduced from six to three thus enhancing the computational efficiency and reducing the numerical dispersion. In the SSCN, all stubs are removed by allowing all six link line impedances to be different [9-10].

In the SSCN, the set of equations (2.15.a - f) are solved for the six link line impedances  $Z_{xy}$ ,  $Z_{xz}$ ,  $Z_{yx}$ ,  $Z_{yz}$ ,  $Z_{zx}$ ,  $Z_{zy}$ . The maximum allowable time step which guarantees all link line impedances are positive can be obtained by solving a third order inequality in  $\Delta t$  given by

$$2 \left( \frac{\Delta t}{\sqrt{\mu\epsilon}} \right)^3 - \left( \frac{\Delta t}{\sqrt{\mu\epsilon}} \right)^2 (S_x + S_y + S_z) - S_x S_y S_z = 0 \quad (2.33)$$

The SSCN has shown substantial improvement in storage, efficiency and maximum allowable time step.

## 2.7 Scattering in a 3-D TLM node

An elegant and simple method for deriving the scattering matrix of a very general TLM node was described in [14] and derived in Appendix A. The method is based on enforcing continuity of the electric and magnetic fields and conservation of charge and magnetic flux. Three equations are derived for the nodal voltages  $V_x$ ,  $V_y$ , and  $V_z$  and another three for the loop currents  $I_x$ ,  $I_y$  and  $I_z$ . From the set of six equations, all the scattered voltages can be obtained. The node voltage in the x direction can be expressed as

$$V_x = \frac{2Y_{yx}(V_{ynx}^i + V_{ypx}^i) + 2Y_{zx}(V_{zpx}^i + V_{znx}^i) + Y_{ox}^i V_{ox}^i}{2Y_{yx} + 2Y_{zx} + Y_{ox} + G_x} \quad (2.34)$$

where the first subscript indicates the direction of propagation and the last indicates polarization, the middle (p or n), if any, indicates a line segment along the positive or negative axis.  $G_x$ ,  $G_y$  and  $G_z$  are the shunt conductances for electric losses in the x, y and z directions respectively.  $Y_{ox}$ ,  $Y_{oy}$  and  $Y_{oz}$  are the characteristic admittances for the shunt open circuited stubs in the x,y and z directions, respectively. Similar expressions for the node voltages in the y and z directions can also be obtained and are given by

$$V_y = \frac{2Y_{xy}(V_{xny}^i + V_{xpy}^i) + 2Y_{zy}(V_{zpy}^i + V_{zny}^i) + Y_{oy}^i V_{oy}^i}{2Y_{xy} + 2Y_{zy} + Y_{oy} + G_y} \quad (2.35)$$

$$V_z = \frac{2Y_{xz}(V_{xnz}^i + V_{xpz}^i) + 2Y_{yz}(V_{ypz}^i + V_{ynz}^i) + Y_{oz}^i V_{oz}^i}{2Y_{xz} + 2Y_{yz} + Y_{oz} + G_z} \quad (2.36)$$

The three loop currents  $I_x$ ,  $I_y$  and  $I_z$  are expressed as

$$I_x = \frac{2(V_{ypz} - V_{ynz}^i + V_{zny}^i - V_{zpy}^i - V_{sx}^i)}{2Z_{yz} + 2Z_{zy} + Z_{sx} + R_x} \quad (2.37)$$

$$I_y = \frac{2(V_{xnz} - V_{xpz}^i + V_{zpx}^i - V_{znx}^i - V_{sy}^i)}{2Z_{xz} + 2Z_{zx} + Z_{sy} + R_y} \quad (2.38)$$

$$I_z = \frac{2(V_{ynx} - V_{ypx}^i + V_{xpy}^i - V_{xny}^i - V_{sz}^i)}{2Z_{xy} + 2Z_{yx} + Z_{sz} + R_z} \quad (2.39)$$

where  $R_x$ ,  $R_y$ , and  $R_z$  are the series resistances for magnetic losses in the x, y and z directions respectively.  $Z_{sx}$ ,  $Z_{sy}$ , and  $Z_{sz}$  are the characteristic impedances for the series short circuited stubs in the x,y and z directions, respectively. The scattered voltages at each node can be obtained by writing expressions in the form



$$V_{ipj} = V_j - I_k Z_{ij} - V_{inj} \quad V_{inj} = V_j + I_k Z_{ij} - V_{ipj} \quad \text{if } j \wedge k = i \quad (2.40)$$

$$V_{ipj} = V_j + I_k Z_{ij} - V_{inj} \quad V_{inj} = V_j - I_k Z_{ij} - V_{ipj} \quad \text{if } j \wedge k = -i \quad (2.41)$$

where any of the subscripts  $i, j$  and  $k$  can be  $x, y$  or  $z$ .

## 2.8 Boundary conditions in TLM

### 2.8.1 The expanded node

#### *Positioning of electric walls*

In the expanded node, short circuits can either be placed half way between two nodes by imposing  $-1$  reflection coefficient or directly through shunt nodes by adding a shunt stub of infinite characteristic admittance to the node. Each shunt node in some plane is responsible for an electric field component perpendicular to the plane. Consequently, to position an electric wall parallel to the  $xy$  plane, which implies all electric field components parallel to that plane must be zero, all the shunt nodes that lie in planes at right angles to the  $xy$  plane must be short circuited.

#### *Positioning of walls of symmetry (magnetic walls)*

walls of symmetry or magnetic walls are always introduced to reduce computational effort. In order to maintain the symmetry of a 3-D TLM node, such walls must run across series nodes. This is achieved by adding a series open circuited stub to all the nodes that lie in planes at right angles to the magnetic wall.

#### *Positioning of dielectric interfaces*

In modeling different media with different constitutive parameters, shunt open circuited stubs are added to shunt nodes or series short circuited stubs are added to series nodes to model each media constitutive parameters, respectively. At the nodes exactly at the interface, the most suitable choice for the stub admittance or impedance is to choose a value that is the average of those used in the two media. However it was found that this choice would considerably increase the storage requirement and hence becomes undesirable from the computational point of view. However, it was found that the error introduced by either stub values from either media is relatively small and acceptable especially when the dielectric are several  $\Delta\ell$  thick, where  $\Delta\ell$  is the cell dimension.

### 2.8.2 Symmetrical condensed nodes

In symmetrical condensed nodes, the boundaries are always placed half way between two adjacent nodes. The link line impedances, open circuited and short circuited stubs are chosen to model the constitutive parameters of the media on both sides of the boundary. Consider two adjacent cells a and b with a boundary placed exactly half way between the two cells. The incident voltage at node b at time step n+1 can be expressed in terms of the reflected voltages at nodes a and b in the previous time step as follows

$${}^{n+1}V_b^i = \rho_{ba} {}^nV_b^r + \tau_{ba} {}^nV_a^i \quad (2.42)$$

where  $\rho_{ba} = \frac{Z_a - Z_b}{Z_a + Z_b}$  and  $\tau_{ba} = 1 - \rho_b$

$Z_a$  and  $Z_b$  are the link line impedances in medium a and medium b respectively. In the symmetrical condensed node, all link line impedances are chosen to be the same. The constitutive parameters of the medium are modeled by the appropriate choice of the characteristic impedance or admittance of the short circuited or the open circuited stubs, respectively. Consequently there will be no special treatment for the cells at the boundary. In the HSCN and SSCN on the other hand, the link line impedances will be different for different media and hence care must be taken for reflections at the interface by applying equation (2.42) for calculating the reflected voltage in the neighborhood of an interface between two different media.

## 2.9 Absorbing boundary conditions in TLM

In modeling problems that involve wave propagation in an open space such as radiation and scattering problems, a basic difficulty arises in TLM method. This is due to the fact that for this kind of problems, the domain in which the field is required to be calculated is unbounded which would consequently require an unlimited data storage. To overcome this problem, the computational domain is truncated by introducing an artificial boundary. The artificial boundary is enforced to truncate the solution while creating the numerical illusion of an infinite space. Mathematically, absorbing boundaries should be constructed in such a way that they absorb all the electromagnetic waves incident upon them. This is implemented inside a TLM mesh in the form of an algorithm which predicts or updates the outgoing field components at absorbing boundaries. In a TLM formulation, it should predict the reflected impulses from the absorbing boundary. In the following discussion, some of the absorbing boundary conditions that have been employed by either FDTD or TLM or both are reviewed.

### **2.9.1 Bench mark solutions**

In this approach, conventional boundaries are used and are placed far away from the source and observation points. The computation is stopped before reflections from the far end reach the observation points. This can be used for either TLM or FDTD. Although, the results are satisfactory, the method is impractical for most application as it requires large amount of memory and very long computational time.

### **2.9.2 Extrapolation methods**

The basic idea behind extrapolation methods is to be able to predict field values at the absorbing boundaries from known field values inside the computation domain at previous time steps. The relationship between these values has to satisfy the governing wave equation while minimizing the reflected waves as much as possible. Knowing that the waves have to be only outgoing at the absorbing boundary, the appropriate formulas can be constructed to model the absorbing boundary. Two types of extrapolation method will be discussed.

#### **2.9.2 a Integral equation approach**

In this approach, the time domain boundary integral equations, electric field integral equations and magnetic field integral equations are discretized and used to extract the field values at the boundary in terms of field values inside the computational domain at previous time steps. The disadvantage of this method is the fact that the computation involves all the nodes on the contour enclosing the computational domain and hence requires extensive computations. The method has been applied to FDTD and was proven to be able to provide good absorption. The method, up to my knowledge, has not been applied to TLM. However from the equivalence between TLM and FDTD, generally any approach applied to either of TLM or FDTD can be reformulated to fit the other.

#### **2.9.2 b One way equations**

The one way equation is a differential equation that allows the wave to propagate in only certain directions. The procedure can be summarized as follows, the wave equation in three dimension can be written as [15]

$$LU = 0 \tag{2.43}$$

where L is the wave operator and U can be any field component in FDTD or a voltage wave in a TLM mesh. The operator L can be decomposed as follows

$$L^+L^-U = 0 \tag{2.44}$$

where  $L^+ U$  at the boundary allows the wave traveling inward,  $L^- U$  at the boundary exactly absorbs the wave traveling outwards at the boundary surface. Different approximations of the one way wave equation  $L^- U = 0$  result in different absorbing boundary conditions with different quality of absorption. However any of these formulations can be always written in the form

$$U(0, y, z, t) = \sum_i \sum_j \sum_k \sum_n a_{i,j,k,n} U(x-i, y \pm j, z \pm k, t-n) \quad (2.45)$$

In the above expression, the computational domain was assumed to lie in  $x < 0$ , the truncated domain is  $x > 0$  and the absorbing boundary condition is placed at  $x = 0$ . Two approaches to the simplification of the one way wave equation are the Taylor expansion and the Higdon's absorbing boundary conditions. The two approaches have the advantage of being simple and having good absorption quality [15].

- **Taylor Expansion**

Assuming that the wave propagates along the positive  $x$  direction, the wave function  $U(x, y, z, t)$  can be expanded along the plane  $x-ct = \text{constant}$ . The coefficients are then obtained by replacing the differential expressions with finite difference expressions. The approximation resulted in small amount of reflection for angle of incidence below  $55^\circ$  [15]. It was also observed that the quality of absorption was not improved for orders higher than 3. For this reason, 2<sup>nd</sup> and 3<sup>rd</sup> order boundary conditions are always sufficient for either TLM or FDTD

- **Higdon's absorbing boundary condition**

The general expression for the Higdon's absorbing boundary condition is in the form

$$\prod_{i=1}^N \left( \frac{\partial}{\partial x} + \frac{\cos(\phi_i)}{c} + \alpha_i \right) U(x, y, z, t) = 0 \quad (2.46)$$

where  $\phi_i$  and  $\alpha_i$  are parameters representing angle of incidence and wave attenuation respectively. An  $N^{\text{th}}$  order boundary condition consists of  $N$  first order boundary operator each having its own parameters  $\phi_i$  and  $\alpha_i$ . The attenuation constant and the angle of incidence might be frequency dependent. In this case, if  $N$  pairs of  $(\phi_i$  and  $\alpha_i)$  can be selected at appropriate frequencies, it is possible to have the Higdon's absorbing boundary condition perform well over a wide range of frequencies. The main advantage of the Higdon's boundary condition is that it does not only absorb propagating waves but evanescent waves as well. This is done by choosing some of the operator parameters  $(\phi_i$  and  $\alpha_i)$  to absorb propagating waves, while others to absorb evanescent modes. For this reason, the Higdon's absorbing boundary condition was claimed to be the most general and optimum representation among absorbing boundary conditions. The only draw back of the Higdon's absorbing boundary condition is that the choice of the boundary parameters are mode and geometry dependent.

The Higdon's absorbing boundary condition has been applied to both TLM and FDTD and was found to give good quality absorption. The coefficients modeling the boundary condition can be obtained using finite difference approximation for the differential equations .

### ***2.9.3 Discrete Green's function approach (Johns Matrix)***

The concept of discrete Green's function was first introduced by *P. B. Johns* and further enhanced by *Hoefler* [16]. The John's matrix is the response of the TLM mesh to a unit impulse excitation at selected input points. The response of the mesh to an arbitrary excitation can be obtained by convolving the excitation with the John's matrix. The technique can be applied to model absorbing boundaries, especially in guided wave structures. The John's matrix of an absorbing boundary for a wave guide structure can be obtained by simulating a waveguide section which is long enough to guarantee that reflections from the far end cannot return to the input reference plane before the computation is stopped. In order to reduce computational time and storage, gradually increasing losses can be introduced to the waveguide section to gradually attenuate the wave as it propagates into the waveguide section. The length and loss profile are optimized to keep the reflections as small as possible in the frequency range of interest [15]. Once the John's matrix of the lossy region is calculated, it can be used for matched termination in further simulations. The Johns matrix approach has been originally developed for TLM application.

### ***2.9.4 Dissipation techniques and perfectly matched layers***

In this approach, a narrow region is constructed just outside the computation domain. In this region, gradual dissipation is introduced in such a way that waves incident on such a boundary are damped on their way in, reflected by a conventional boundary condition and then damped further in their way back.

The technique was first explored in a TLM In [17], a matched termination for a waveguide structure was implemented with a waveguide section with gradually increasing losses. The loss tangent profile and the length of the lossy section were optimized to guarantee minimum reflections in the frequency range of interest. This was done with the aid of Touchstone CAD software. A return loss of less than -32 dB was observed.

Recently, a new concept for designing a perfectly matched layer PML has been proposed for FDTD [18]. The PML has both magnetic and electric loss components. By properly associating different electric or magnetic conductivities to different field components, it was shown that the PML theoretically would not cause any reflection at an interface with free space for incident fields at any frequency and any angle of incidence. The conductivities are chosen to vary continuously with space in order to minimize numerical reflections. In [19], it was shown that the PML is very effective in absorbing TEM and quasi TEM waves as well as non TEM waves above their cutoff frequencies. However for evanescent waves, it cannot

provide any more attenuation and hence become ineffective in absorbing these kind of waves. For this reason, special care must be taken in placing PML away from any discontinuity where evanescent modes are most likely to exist.

## **2.10 Summary**

This chapter included a review of the time domain TLM. The two dimensional series and shunt nodes were analyzed. The development of three dimensional nodes was then discussed, starting from the expanded node to improved condensed nodes that were able to overcome the difficulties associated with the expanded node. This included the SCN, a pair of HSCN and the SSCN. The choice of the link line impedances/admittances of each of these nodes was discussed. The characteristic impedances or admittances of the compensating short circuit or open circuited stubs were also derived for each of these nodes. Scattering in a general symmetrical condensed node was also derived. In this chapter the boundary treatment in a TLM mesh was discussed. This included different kind of boundaries as well absorbing boundary conditions.